ZD4054, a specific antagonist of the endothelin A receptor, inhibits tumor growth and enhances paclitaxel activity in human ovarian carcinoma *in vitro* and *in vivo*

Laura Rosanò,[1] Valeriana Di Castro,[1] Francesca Spinella,[1] Maria Rita Nicotra,[3] Pier Giorgio Natali,[1,2] and Anna Bagnato[1]

[1]Molecular Pathology and [2]Immunology Laboratories, Regina Elena Cancer Institute, Via delle Messi d'Oro, [3]Molecular Biology and Pathology Institute, National Research Council, Rome, Italy

Abstract

The autocrine endothelin (ET)-1/endothelin A receptor (ET_AR) pathway is an important regulator of several processes involved in ovarian cancer progression, and its overexpression is associated with aggressive disease. These features have led to the proposal of the ET_AR receptor as a potential target for improving ovarian cancer treatment. In this study, we evaluated *in vitro* and *in vivo* the effects of ZD4054, an orally active antagonist that specifically binds ET_AR, as monotherapy, and in combination with paclitaxel. In the human ovarian cancer ET_AR-positive cell lines HEY, OVCA 433, SKOV-3, and A-2780, ZD4054 effectively inhibited the basal and ET-1–induced cell proliferation, associated with the inhibition of AKT and p42/44MAPK phosphorylation, and with increased apoptosis, through the inhibition of bcl-2 and activation of caspase-3 and poly(ADP-ribose) polymerase proteins. ZD4054 treatment also resulted in a reduction of ET_AR-driven angiogenesis and invasive mediators, such as vascular endothelial growth factor, cyclooxygenase-1/2, and matrix metalloproteinase (MMP). The combination of ZD4054 and paclitaxel led to the potentiation of all these effects, indicating that ZD4054, by blocking the ET_AR-dependent proliferative, invasive, and antiapoptotic signals, can enhance sensitivity to paclitaxel. In HEY ovarian cancer xenografts, ZD4054 significantly inhibited tumor growth to the same degree as paclitaxel. Furthermore, ZD4054-dependent tumor growth inhibition was associated with a reduction in proliferation index, microvessel density, and MMP-2 expression. Interestingly, the combination of ZD4054 and paclitaxel produced additive antitumor effects, with 40% of mice remaining tumor-free, supporting a rationale for the clinical use of ZD4054 as monotherapy or in combination with cytotoxic drugs. [Mol Cancer Ther 2007;6(7):2003–11]

Introduction

Among gynecologic malignancies, epithelial ovarian carcinoma is associated with the highest mortality rate in the Western world. Most cases are diagnosed at an advanced stage of the disease resulting into a poor survival rate (1). Although chemotherapy regimens are associated with high remission rate, the disease frequently relapses with drug resistance being a significant barrier to cure (2). To overcome the limitations of cytotoxic chemotherapies, current approaches to drug design in oncology are aimed at modulating specific cell signaling pathways relevant to tumor growth and survival. In this context, clinical trials evaluating targeted therapy have indicated that improved survival can be achieved through combination schedules with chemotherapy. Although cancer cells integrate multiple signaling pathways sustaining tumor progression, therapeutic interest in the endothelin-1 (ET-1) axis is supported by its central role in several human cancers, including ovarian carcinoma (3–6). ET-1 is a member of the endothelin family of three closely related isopeptides, ET-1, ET-2, and ET-3. Two major receptor subtypes that mediate ET's biological effects belong to the G-protein coupled receptor family: the ET_A receptor (ET_AR) is considered as the major effector of the ET axis and binds ET-1 and ET-2 with high affinity and ET-3 with low affinity; whereas the ET_BR binds all ET isopeptides with the equal affinity (7). Interestingly, in gene expression profiles of late-stage ovarian cancer, ET_AR was identified as a metastasis-associated gene that activates cell signaling involved in the control of cell migration, spread, and invasion (8, 9). Levels of ET-1 are markedly elevated in the ascites of patients with epithelial ovarian cancer (10) and, together with the ET_AR, are overexpressed and activated in 85% of ovarian tumors, correlating with advanced stages (7, 11, 12). In ovarian cancer cells, the autocrine loop mediated by the ET-1/ET_AR receptor-ligand interaction has been implicated in the parallel activation of several signal transduction pathways, including Ras/Raf/mitogen-activated protein kinase (MAPK), phosphoinositide-3-kinase (PI3K)–dependent integrin-linked kinase and AKT activation, Src-mediated epidermal growth factor receptor transactivation, and p125 focal adhesion kinase and paxillin modulation (8, 13–15). This cascade of events ultimately induces nuclear transcription of several proto-oncogenes,

Received 3/5/07; revised 5/4/07; accepted 5/25/07.

Grant support: Associazione Italiana Ricerca Sul Cancro, Ministero della Salute.

The costs of publication of this article were defrayed in part by the payment of page charges. This article must therefore be hereby marked *advertisement* in accordance with 18 U.S.C. Section 1734 solely to indicate this fact.

Requests for reprints: Anna Bagnato, Molecular Pathology Laboratory, Regina Elena Cancer Institute, Via delle Messi D'Oro 156, 00158 Rome, Italy. Phone: 39-6-52662565; Fax: 39-6-52662600.
E-mail: bagnato@ifo.it

doi:10.1158/1535-7163.MCT-07-0151

promoting cell proliferation and escape from apoptosis, neovascularization, protease production, epithelial-to-mesenchymal transition, and invasiveness, suggesting that ET-1 may also play a role in metastatic competence (6, 12, 16–20). Interestingly, ET-1 protects ovarian cancer cells from paclitaxel-induced apoptosis via a bcl-2–dependent mechanism and involves the activation of AKT. This survival pathway is inhibited by ET_AR antagonists, indicating that ET_AR blockade could increase the commitment toward apoptosis induced by paclitaxel (16). Importantly, pharmacologic blockade of the ET_AR inhibits tumor xenograft growth and molecular determinants involved in tumor progression (11–13, 21). The pleiotropic effects exerted by ET-1 in the development of ovarian cancer and other epithelial tumors, such as prostate and cervical cancers, has led to the development of small molecules that antagonize the binding of ET-1 to the ET_AR (22–24). Among various ET_AR antagonists, ZD4054 is an orally active ET_AR antagonist in early clinical development for the treatment of cancer. The synthesis and molecular characterization of ZD4054 has been described previously (25). ZD4054 binds to the ET_AR with high affinity. In preclinical studies, ZD4054 specifically antagonizes ET_A-mediated proliferative and antiapoptotic effects, but not ET_B-mediated proapoptotic effects in different cell types (26, 27). We have demonstrated previously that in ovarian cancer cells, ZD4054 antagonizes ET-1–induced cell proliferation (27). Given the encouraging preliminary results, in this study, we investigated the antitumor activity of ZD4054 in ovarian carcinoma by a multiparametric analysis *in vitro* and *in vivo*. The effects of ET_AR antagonism described above, together with evidence of protection against paclitaxel-induced apoptosis, provided the rationale for evaluating the therapeutic activity of ZD4054 in combination with conventional chemotherapeutic agents (16). Preclinical studies using a combination treatment of ET_AR antagonist with paclitaxel revealed additive therapeutic efficacy in ovarian, cervical, and prostate carcinomas (21, 22, 28–30). Therefore, we determined *in vitro* and *in vivo* the relative contributions of ZD4054 administered alone or in combination with paclitaxel to the inhibition of basal cell proliferation and apoptosis protection. Our findings provided mechanism-based evidence demonstrating that *in vitro* and *in vivo*, ZD4054, by blocking the ET-1/ET_AR axis and its related signaling cascade, displayed several antitumor activities that were of the same magnitude of effect as paclitaxel. Furthermore, combined ZD4054 and paclitaxel treatment resulted in a greater degree of inhibition of tumor growth and tumor-promoting effects compared with single agents.

Materials and Methods

Materials

Clinical grade ZD4054, *N*-(3-methoxy-5-methylpyrazin-2-yl)-2-(4-[1,3,4-oxadiazol-2-yl]phenyl)pyridine-3-sulfonamide, was kindly provided by AstraZeneca (Macclesfield, UK). Paclitaxel was kindly provided by Bristol Myers (Sermoneta, Italy).

Cells and Cell Culture Conditions

Human ovarian carcinoma cell lines, HEY, OVCA 433, and A-2780, were a generous gift from Dr. Giovanni Scambia (Catholic University School of Medicine, Rome, Italy). The SKOV-3 cell line was obtained from the American Type Culture Collection. All culture reagents were from Invitrogen. The cells were serum starved by incubation for 24 h in serum-free DMEM. ET-1 (Peninsula Laboratories) was used at 100 nmol/L and incubated with the cells for the indicated times. Pretreatment of cells with ZD4054 was performed for 30 min prior to the addition of ET-1.

Thymidine Incorporation Assay

Serum-starved HEY, OVCA 433, SKOV-3, and A-2780 cells were treated with ZD4054 (1 μmol/L) and/or paclitaxel (60 nmol/L), and after 24 h, 1 μCi of [methyl-^{3}H]-thymidine (5 Ci/μmol/L) was added to each well. The thymidine incorporation assay was performed as described previously (21). Responses to all treatments were assayed in sextuplicate, and results were expressed as the means of three separate experiments.

ELISA

Serum-starved HEY cells were treated for 24 h with 1 μmol/L ZD4054 or 60 nmol/L paclitaxel or in combination. The vascular endothelial growth factor (VEGF) protein levels in the cell-conditioned media were determined in triplicate by ELISA using the Quantikine human VEGF immunoassay kit (R&D Systems). The sensitivity of the assay is less than 5.0 pg/mL. Intra-assay variation is 5.4%, and interassay variation is 7.3%. Gelatinase activities in conditioned medium were determined by a matrix metalloproteinase (MMP) gelatinase activity assay kit (Chemicon) according to the manufacturer's instructions. The sensitivity of the assay is <5 ng/mL MMP in the range 10–200 ng/mL.

Apoptosis Assay

The induction of programmed cell death was determined as described previously (16) by the cell death detection ELISA Plus kit (Boehringer Mannheim). Briefly, 5×10^4 cells per well were seeded into 12-well plates. After a 48-h treatment, cells were lysed, and the supernatants were recovered and assayed for histone-associated DNA fragments, as recommended by the manufacturer, at 405 nm by the use of a microplate reader. The experiments were performed in quadruplicate and repeated twice. For detection of early apoptotic events, nonadherent and adherent cells were collected. Cells (1×10^6) were double stained with FITC-conjugated annexin-V and propidium iodide using the Vybrant apoptosis kit according to the manufacturer's instructions (Molecular Probes) and analyzed by cytofluorometric analysis.

Western Blot Analysis

For protein detection, whole cell lysates were subjected to SDS-PAGE and revealed by Western blotting using antibodies to caspase-3, phospho-AKT and AKT, phospho-p42/44 MAPK, and p42/44 MAPK (Cell Signaling), bcl-2 and poly(ADP-ribose) polymerase (PARP) (Santa Cruz Biotechology, Inc.), cyclooxygenase-1 (COX-1) and COX-2

(Cayman Chemical). Blots were developed with the enhanced chemiluminescence detection system (ECL; Amersham Pharmacia Biotech). The membranes were reprobed with anti–β-actin antibody to ascertain that an equal amount of protein from cell extracts was analyzed (Oncogene, CN Biosciences, Inc.).

Gelatin Zymography

The HEY cell supernatants were electrophoresed for analysis in 9% SDS-PAGE gels containing 1 mg/mL gelatin as previously described (19). Briefly, the cells were washed for 30 min at 22°C in 2.5 % Triton X-100 and then incubated in 50 mmol/L Tris (pH, 7.6), 1 mmol/L $ZnCl_2$, and 5 mmol/L $CaCl_2$ for 18 h at 37°C. After incubation, the gels were stained with 0.2% Coomassie blue. Enzyme-digested regions were identified as white bands on a blue background.

Xenografts in Nude Mice

Female athymic (nu^+/nu^+) mice, 4–6 week of age (Charles River Laboratories) were treated following the guidelines for animal experimentation of the Italian Ministry of Health. Mice were injected s.c. into one flank with 1.5×10^6 viable HEY cells. After 7 days, when tumors reached approximately 0.2–0.3 cm in diameter, mice were randomized in groups ($n = 10$) to receive different treatments. One group was treated i.p. for 21 days with ZD4054 (diluted in PBS) at the indicated daily doses (10, 25, or 50 mg/kg/day). Control mice were injected i.p. with vehicle. To compare the effects of ZD4054 and paclitaxel treatment, three different experiments with a total of 30 mice for each experiment were performed. One group was treated i.p. for 21 days with ZD4054 at 25 mg/kg/day, one group with paclitaxel (three 20 mg/kg i.v. doses every 4 days, diluted in PBS), and control mice i.p. with 200 μL drug vehicle. For the combination treatment of ZD4054 and paclitaxel, one group was treated i.p. for 21 days with ZD4054 at the dose of 10 mg/kg/day; one group was treated i.v. with paclitaxel 20 mg/kg given three times every 4 days (diluted in PBS), one group with ZD4054 in combination with paclitaxel and control mice i.p. with 200 μL drug vehicle and 200 μL drug vehicle i.v. as scheduled for the paclitaxel. On day 40 after tumor injection, tumors were removed from control and treated mice and snap frozen for immunohistochemical analysis. Tumor size was measured with calipers and was calculated using the formula $\pi/6 \times$ larger diameter $\times$ [smaller diameter]^2.

Immunohistochemical Analysis

Indirect immunoperoxidase stain of tumor xenografts was performed on acetone-fixed 4-μm tissue sections as described previously (21). Briefly, sections were incubated with monoclonal rat anti-mouse CD31 [platelet/endothelial cell adhesion molecule 1 (PECAM-1); generously donated by Dr. A Mantovani, Mario Negri Institute, Milan, Italy], anti–MMP-2 (Oncogene), and anti–Ki-67 monoclonal antibody (clone MIB1; Ylem). The avidin-biotin assays were performed using the Vectastain Elite kit (for nonmurine primary antibodies) and Vector MOM immunodetection kit (for murine primary antibodies) obtained from Vector Laboratories. Mayer's hematoxylin was used as a nuclear counterstain. Negative control stain was represented by sections in which the incubation with the primary antibody was either omitted or substituted by isotype-matched immunoglobulins. The evaluation of microvessel density was performed by two independent observers on an ×200 field according to the criteria of Weidner et al. (31). Cells positive for Ki-67 were expressed as the percentage of tumor cells with nuclear staining counted in three separate ×40 microscopic fields (at least 200 cells per field were counted).

Statistical Analysis

Statistical analysis was performed using Student's t test and Fisher's exact test as appropriate. The time course of tumor growth was compared across the groups using two-way ANOVA, with group and time as variables. All statistical tests were carried out using SPSS software (SPSS). A two-sided probability value of <0.05 was considered statistically significant.

Results

Cell Proliferation Inhibition by ZD4054 and Paclitaxel

The potential antiproliferative effect of ZD4054 alone or in combination with paclitaxel was evaluated on HEY, OVCA 433, SKOV-3, and A-2780 cells that release ET-1 and express functional ET_AR (4, 5). The ET-1 levels released from these cells were within the physiological range needed for the activation of the ET_AR in an autocrine fashion (12). Serum-starved cell lines were exposed to ZD4054 (1 μmol/L) and/or paclitaxel (60 nmol/L). As measured by the [^{3}H]-thymidine incorporation assay, significant inhibition of cell proliferation was observed in ZD4054-treated cells (Fig. 1A). Furthermore, combination of ZD4054 and paclitaxel led to a greater inhibition of cell growth induced by endogenous ET-1 in comparison to the partial inhibition produced by single agents. This observation suggests that the specific blockade of the ET_AR with ZD4054 cooperates with conventional cytotoxic drugs, such as paclitaxel, to inhibit ovarian tumor growth (Fig. 1A). Similar results were obtained in the presence of exogenous ET-1 (Supplementary Fig. S1).[4] Because inhibition of cell growth could also be due to the induction of apoptosis induced by ZD4054 or taxol, we therefore investigated whether ZD4054 could potentiate the effect of paclitaxel by inducing apoptosis compared with either single agent. ET_AR activation by ET-1 triggers multiple signal transduction pathways that include MAPK and AKT pathways (8, 15). In particular, we previously demonstrated that PI3K-dependent Akt pathway has a central role in ET_AR-mediated protection against paclitaxel-dependent apoptosis in ovarian cancer cells (16). Therefore, we evaluated whether ZD4054 treatment was associated with reduced ET_AR-driven downstream signaling pathway in HEY cells. As expected, serum-starved HEY cells displayed constitutive levels of activated AKT and p42/44 MAPK; the addition of exogenous ET-1 induced a marked increase in the phosphorylation of p42/44 MAPKs and

[4] Supplementary material for this article is available at Molecular Cancer Therapeutics Online (http://mct.aacrjournals.org/).

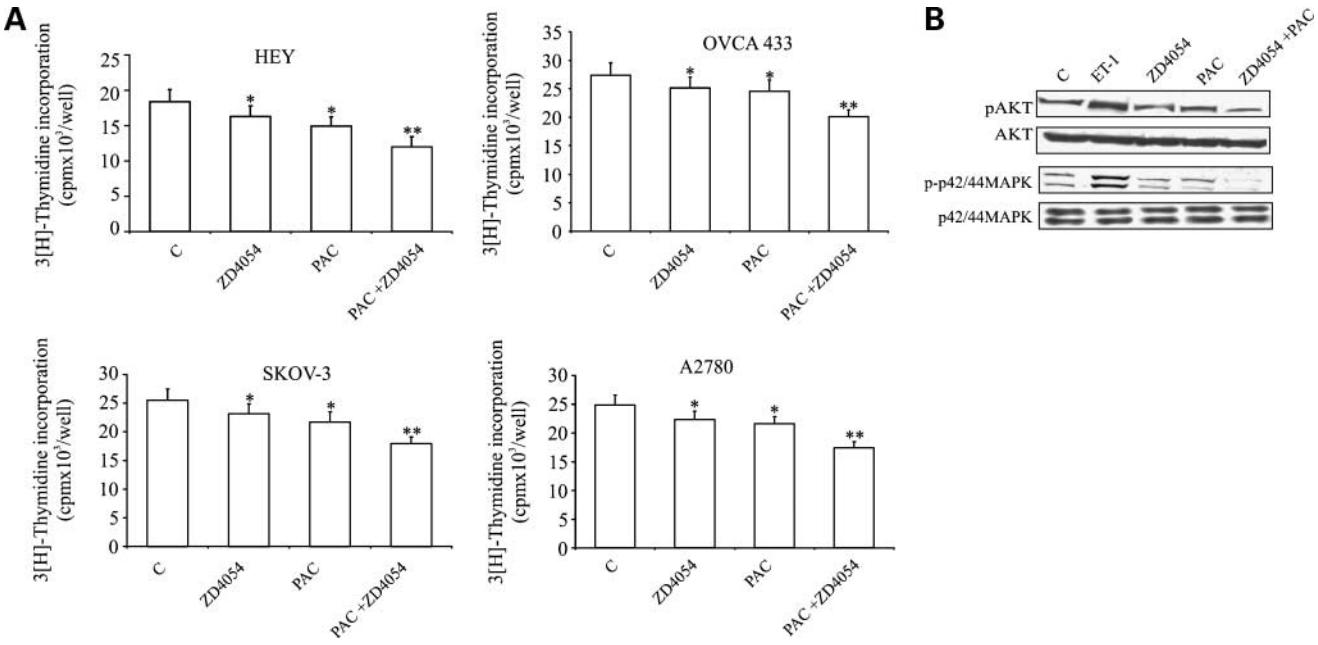

Figure 1. Effect of ZD4054 in monotherapy and combination therapy with paclitaxel on ovarian carcinoma cell proliferation and on MAPK and AKT signaling pathways. **A,** serum-starved HEY, OVCA 433, SKOV-3, and A-2780 cells were treated with ZD4054 (1 μmol/L) or paclitaxel (*PAC*, 60 nmol/L) or ZD4054 + PAC before measuring [^{3}H]-thymidine incorporation. *Columns,* averages of sextuplicate determinations of three separate experiments; *bars,* SD; *, $P < 0.001$ compared with control (*C*); **, $P < 0,0001$ compared with ZD4054 or paclitaxel. **B,** whole-cell lysates of HEY cells treated with ET-1 (100 nmol/L) or with ZD4054 (1 μmol/L) or paclitaxel (60 nmol/L) or ZD4054 + paclitaxel were blotted for detection of total and activated p42/44 MAPK and AKT by using specific antibodies.

AKT, as assessed by the use of specific antibodies (Fig. 1B). ZD4054 decreased the endogenous ET-1–induced phosphorylation/activation of both kinases, and combination of ZD4054 with paclitaxel exerted a stronger interruption of the two signaling pathways (Fig. 1B). Together, these data suggest that ZD4054, as monotherapy and in combination with paclitaxel, affected ET_AR-dependent signal transduction pathways related to cell proliferation and survival.

Effect on Apoptosis

To determine whether the growth-inhibitory effect of ZD4054 could involve the induction of apoptosis, HEY and OVCA 433 cells were treated with ZD4054 or paclitaxel for 48 h and evaluated by ELISA assay, which detected histone-associated DNA fragments. As shown in Fig. 2A, ZD4054 was able to induce an increase in apoptotic cells similar to that induced by paclitaxel ($P < 0.01$ compared with control). The combined treatment of ZD4054 plus

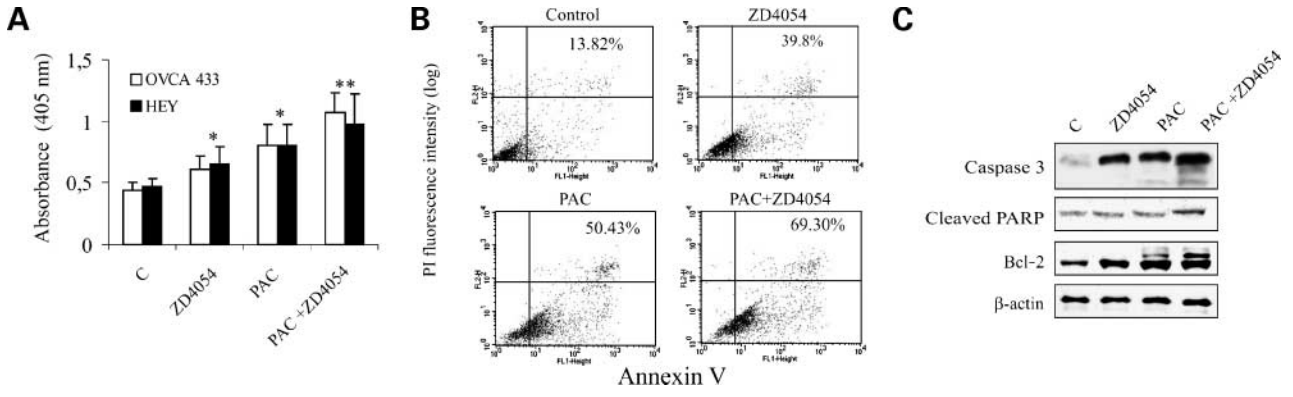

Figure 2. Induction of apoptosis by treatment with ZD4054 and paclitaxel in ovarian carcinoma cells. **A,** HEY and OVCA 433 cells were treated for 48 h with ZD4054 (1 μmol/L) or with paclitaxel (*PAC*, 60 nmol/L) or in combination (*PAC + ZD4054*). *Columns,* averages of quadruplicate determinations of two separate experiments; *bars,* SD. *, $P < 0.01$ compared with control (*C*); **, $P < 0.001$ compared with ZD4054 or paclitaxel. **B,** apoptotic changes induced by exposure of HEY cells treated as in **A**, were determined by flow-cytometric analysis of annexin V – propidium iodide staining. **C,** cell lysates of serum-starved HEY cells treated as in **A** were processed for Western blot using antibodies capable of recognizing the proforms and activated forms of caspase-3, PARP, and bcl-2. The membranes were probed with anti – β-actin antibody to ensure equal amount of proteins.

paclitaxel markedly increased apoptosis ($P < 0.001$ compared with ZD4054 or paclitaxel alone). HEY cells were also analyzed for the presence of early apoptotic events using annexin V staining (Fig. 2B). Treatment of serum-starved HEY cells with ZD4054 increased the number of early apoptotic cells from ~13% to ~39%, confirming our previous findings that, in ovarian cancer cells, endogenous ET-1 induces survival signaling through the ET_AR (15). The coadministration of ZD4054 significantly potentiated (~70%, $P < 0.005$ compared with single agent treatment) the cytotoxic drug-induced apoptotic cell death in an additive manner, suggesting a specific therapeutic window in which combination therapy may be more effective at inducing apoptotic death in ovarian cancer cells. In view of the described effects on apoptosis induction, we examined the effects of ZD4054 on the levels of apoptosis-related protein expression. Treatment of HEY cells with either ZD4054 or paclitaxel alone resulted in little or no detectable cleaved caspase-3. In contrast, combination treatment resulted in the accumulation of processed caspase-3. Moreover, combination treatment also resulted in increased cleaved PARP, a substrate of activated caspase-3, compared with single agents (Fig. 2C), suggesting that paclitaxel and ZD4054 act in a cooperative fashion to activate apoptosis through a caspase-dependent pathway. As commitment to apoptosis is largely a mitochondrial event, controlled by antiapoptotic proteins in the bcl-2 family, we also investigated whether ZD4054 could modulate the expression of bcl-2 induced by paclitaxel. As shown in Fig. 2C, although paclitaxel treatment induced a significant increase in phosphorylation and, thus, inactivation of bcl-2, the addition of ZD4054 potentiated the paclitaxel-induced effect, confirming the potential cooperation of ZD4054 to enhance the therapeutic efficacy of paclitaxel.

Inhibition of Invasion and Angiogenesis

We have demonstrated previously that the tumor-promoting effects of ET-1 through the ET_AR in ovarian carcinoma cells also includes the secretion and activation of MMPs, such as MMP-2 and MMP-9, which are highly relevant in angiogenesis as well as in tumor cell invasion and metastasis (18, 19). Thus, we investigated whether ZD4054 may inhibit ET-1–induced MMP secretion and activity in ovarian carcinoma cells. Both gelatin zymography and activity measurements demonstrated an increase in MMP-2 and MMP-9 activity after 48 h in ET-1–stimulated HEY cells. Pretreatment with ZD4054 reduced the basal MMP activity (Fig. 3A and B), and this effect was more pronounced when ZD4054 was added in combination with paclitaxel. In ovarian carcinoma cells, ET-1 increases VEGF, COX-1, and COX-2 expression through the ET_AR, and these modulate invasive behavior (17, 18). Therefore, we also tested the therapeutic efficacy of ZD4054 alone or in combination with paclitaxel on the endogenous production of VEGF and on COX-1/-2 expression. By ELISA assay, we found that ZD4054 inhibited basal production of VEGF by ~30% (comparable to the effect seen with paclitaxel), confirming the involvement of an autocrine $ET\text{-}1/ET_AR$ in this effect (Fig. 3C). This inhibitory effect was more evident in the presence of both drugs (reaching ~60%), indicating that combination therapy was also effective in preventing endogenous ET-1–induced production

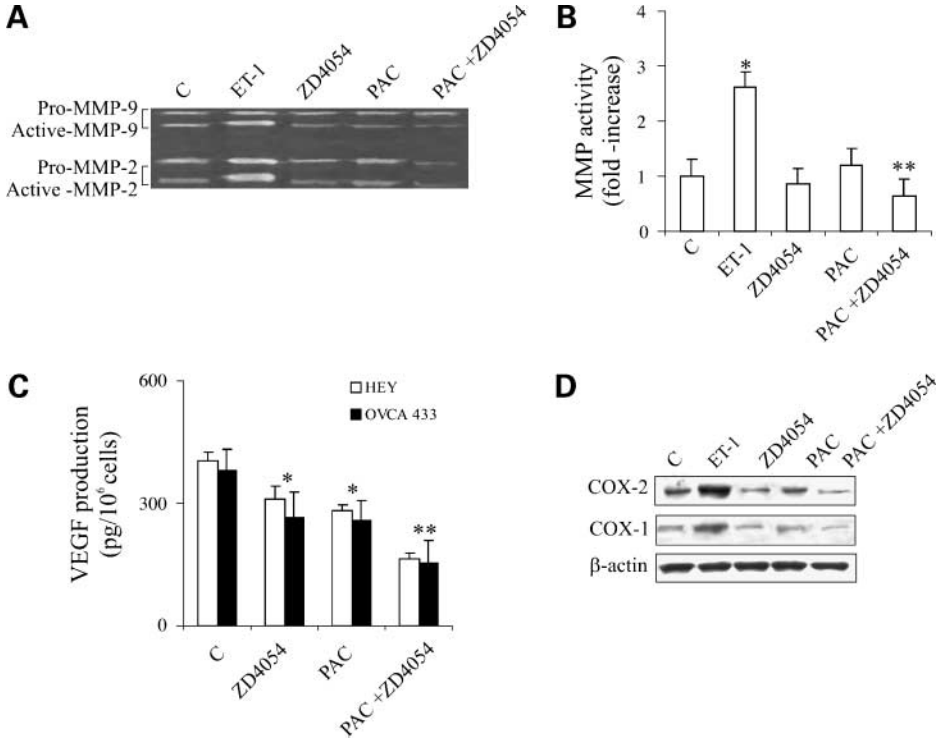

Figure 3. Effects of ZD4054 in monotherapy and combination therapy with paclitaxel on ovarian carcinoma cell angiogenesis and invasion. **A,** serum-starved HEY cells were treated with ET-1 (100 nmol/L) or ZD4054 (1 μmol/L) or paclitaxel (*PAC*, 60 nmol/L) or in combination (PAC + ZD4054) for 48 h. Gelatin zymography was used to determine the activities of MMP-2 and MMP-9. **B,** MMP activity was also measured by a MMP gelatinase activity assay kit. *Bars,* SD; *, $P < 0.05$ compared with the control (*C*); **, $P < 0.001$, compared with ZD4054 or paclitaxel. **C,** VEGF production measured in HEY and OVCA 433 cells treated as in **A** is reported as means of results from three ELISA determinations, each performed in duplicate. *Bars,* SD; *, $P < 0.001$ compared with control; **, $P < 0.001$ compared with ZD4054 or paclitaxel. **D,** cell lysates of serum-starved HEY cells, treated as in **A**, were analyzed for COX-1 and COX-2 protein expression by Western blotting and reprobed with anti–β-actin antibody to ensure equal amount of proteins.

of VEGF leading to tumor neovascularization. Moreover, ET-1 significantly induced COX-1 and COX-2 protein upregulation. Basal COX-1/-2 was inhibited by both ZD4054 and paclitaxel, and this effect was more significantly inhibited when ZD4054 was added in combination with paclitaxel compared with either agent (Fig. 3D). Taken together, these results indicate that ZD4054 alone, and to a greater extent in combination with paclitaxel, reduced the expression of angiogenic and invasive mediators, such as MMPs, VEGF, and COX-1/-2 induced by endogenous ET-1, in ovarian carcinoma cells leading to an inhibition of tumor progression.

Inhibition of Growth of Human HEY Ovarian Carcinoma in Nude Mice

The potential antitumor effect of ZD4054 *in vivo* was assessed in murine tumor xenografts. Human HEY cells were grown as s.c. tumors in nude mice. Following 7 days of tumor growth, when established xenografts were palpable, mice were treated with three different doses of ZD4054 i.p. for 21 days: 10, 25, and 50 mg/kg/day. Treatment with ZD4054 produced a 69% inhibition of tumor growth on day 40 after tumor injection, with either medium (25 mg/kg/day) or high (50 mg/kg/day) doses (both $P < 0.001$ compared with control; Fig. 4A). ZD4054 treatment was generally well tolerated, with no detectable signs of acute or delayed toxicity, even at the highest dose. As shown in Fig. 4B, the tumor growth inhibition obtained with ZD4054 (25 mg/kg/day) treatment was comparable with that achieved with paclitaxel (three 20 mg/kg i.v. doses every 4 days). We next evaluated whether the cooperative effects of ZD4054 and paclitaxel *in vitro* could also be present *in vivo*. A marked and sustained growth inhibitory effect was observed when ZD4054 (10 mg/kg/day) was used in combination with paclitaxel (three 20 mg/kg i.v. doses every 4 days), causing significant inhibition in tumor growth at the end of the 4-week treatment period in all mice (87%, $P < 0.002$) when compared to mice treated with a single agent. The comparison of the time course of tumor-growth curves by two-sided ANOVA, using group and time as variables, showed that the group-by-time interaction for tumor growth was statistically significant ($P < 0.0001$; Fig. 5A). As shown in Table 1, the combined treatment was highly effective, with no histological evidence of HEY tumors in 4 out of 10 mice. The combination treatment at the dose and schedule tested was well tolerated, as indicated by the absence of weight loss or other signs of acute or delayed toxicity. Moreover, as shown by Fig. 5A, the tumor growth inhibition obtained with combination treatment of ZD4054 and paclitaxel persisted for up to 4 weeks after termination of treatment. To demonstrate that the inhibition of tumor growth observed in treated mice was accompanied by a significant reduction in tumor cell proliferation and vascularization, tissue sections of HEY tumors on day 40 after tumor cell injection were analyzed by immunohistochemistry (Fig. 5B and Table 1). Tumor-induced vascularization, quantified by staining of tissue sections with an anti-CD31 antibody, was significantly reduced versus controls, following treatment with either ZD4054 or paclitaxel (~60% and ~54%, respectively; $P < 0.05$ compared with control). Moreover, in mice treated with ZD4054 plus paclitaxel, this inhibition reached ~75% ($P < 0.002$ compared with single agents). The inhibition of tumor vascularization was associated with the inhibition of the expression of MMP-2 in all treatment schedules (data not shown). We also found that the number of proliferating tumor cells, measured by the number of Ki-67–positive cells, was reduced from 37.3 ± 1.5 in tumors of control mice to 22.4 ± 3.3 and 27.7 ± 2.2 in tumors of mice treated with either ZD4054 or paclitaxel, respectively ($P < 0.05$ compared with control), whereas in the combination therapy group, the number of Ki-67–positive cells was reduced to 15.7 ± 3.3 ($P < 0.002$ compared with single agents).

Discussion

In recent years, many experimental studies have been performed to develop novel antitumor agents that are capable of selectively interfering with key oncogenic signaling pathways. The ET_AR has been reported as a

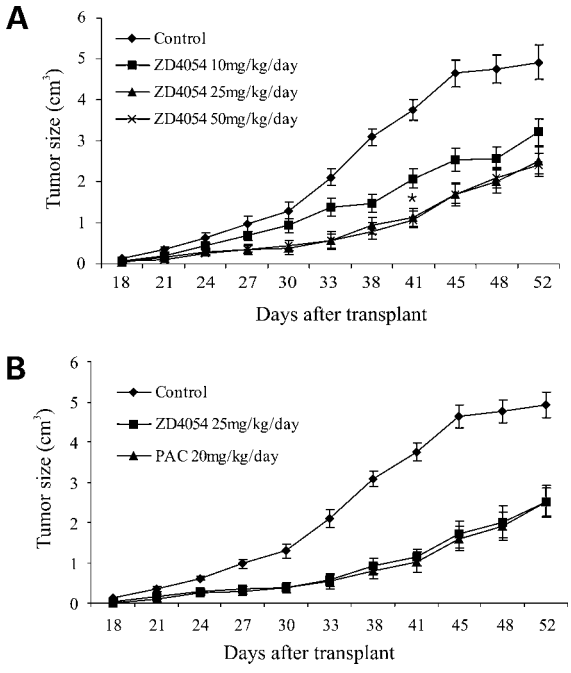

Figure 4. Antitumor activity of ZD4054 and paclitaxel on established HEY human ovarian carcinoma xenografts. **A,** mice were given injections of 1.5×10^6 HEY cells s.c. into the dorsal flank. After 7 d, mice were treated i.p. for 21 d with vehicle (*Control*), and three doses of ZD4054 (10, 25, or 50 mg/kg/day). Three different experiments using a total of 40 mice for each experiment were performed. In each experiment, each group consisted of 10 mice. Treatment with ZD4054 produced a 69% inhibition of tumor growth on day 40 after tumor injection, with either medium (25 mg/kg/day) or high (50 mg/kg/day) doses ($P < 0.001$ compared with control). Data represent mean tumor volume. **B,** mice bearing HEY tumor xenografts were treated as follows: one group with 25 mg/kg/day of ZD4054 for 21 d, one group with three i.v. administrations of paclitaxel (*PAC*, 20 mg/kg) every 4 d, and one group with vehicle (*Control*). Data represent mean tumor volume.

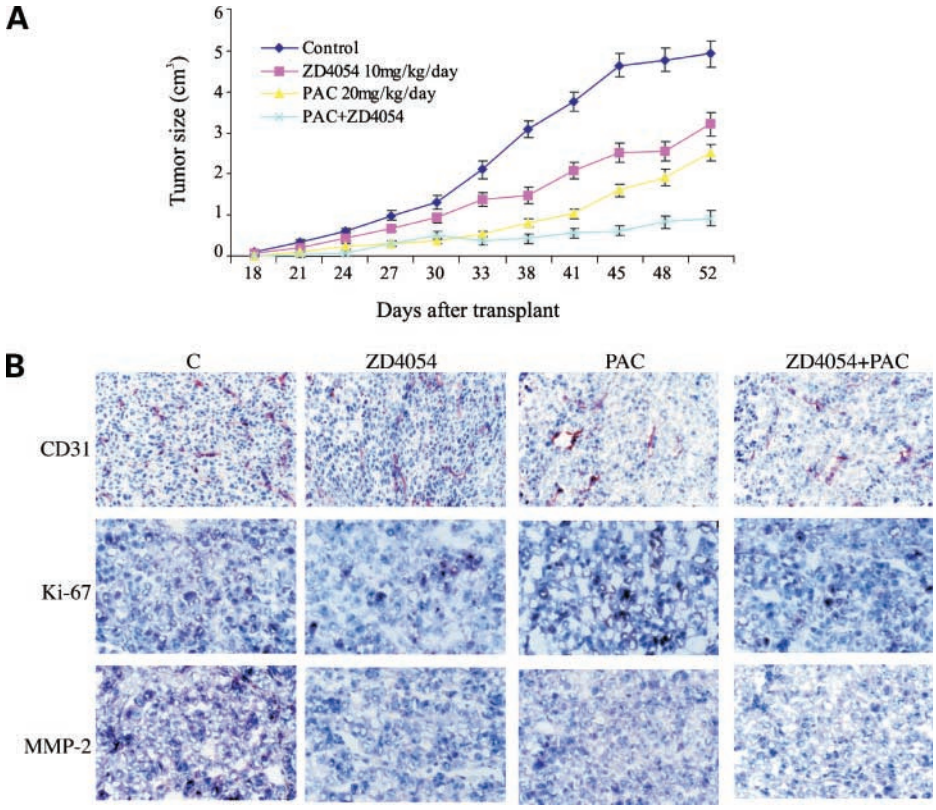

Figure 5. Antitumor activity of ZD4054 treatment in combination with paclitaxel. **A,** mice bearing HEY tumor xenografts were treated as follows: one group received i.p. for 21 d ZD4054 (10 mg/kg/day); one group with paclitaxel (*PAC*, 20 mg/kg/dose given i.v. every 4 d for three doses), and one group was administered with ZD4054 in combination with paclitaxel. The group-by-time interaction for tumor growth was statistically significant ($P < 0.0001$). Data represent mean tumor volume. **B,** immunohistochemical analysis. Tumors removed from controls and treated mice were immunostained for expression of CD31, Ki-67, and MMP-2, as described in the experimental procedures (original magnification, ×200). **C,** control; *PAC,* paclitaxel. This figure shows representative sections taken from each of the appropriate animal groups.

new therapeutic target in several human cancers, including cervical (32), prostate (33), ovarian (21), breast (34), colon (35), lung (36), renal (37), and thyroid gland (38) malignancies. ET_AR signaling has been shown convincingly to regulate stromal-tumor cell interactions promoting tumor growth, neovascularization, and metastatic spread (3, 11, 12, 39). In particular, we have previously demonstrated overexpression of the ET-1/ET_AR autocrine loop in primary and metastatic ovarian carcinomas and its contribution to tumor growth and progression (21). In these malignancies, overexpression of the ET-1 axis is associated with advanced-stage disease and has pleiotropic activities including enhanced migration, invasion, and epithelial-to-mesenchymal transition, which could be reversed by specific blockade of the ET_AR (10–21). In this respect, interfering with ET_AR and its downstream targets may provide an opportunity for the development of new, mechanism-based strategies for cancer treatment, as demonstrated by the preclinical results with small molecules targeting ET_AR (21–24). Thus, we demonstrated previously that *in vivo* inhibition of the ET_AR autocrine pathway using ET_AR antagonism results in growth reduction of tumor xenografts (11–13, 21). In the present study, we demonstrated the therapeutic relevance of the specific ET_AR

Table 1. Immunohistochemical analysis of HEY ovarian carcinoma xenograft after treatment with ZD4054 and paclitaxel

Treatment	Tumor volume (cm^3), mean ± SD	Mice tumor free (*n*)	Median vessel density*	Proliferation index Ki-67†
Control	3.7 ± 1.29	0/10	67 ± 6	37.3 ± 1.5
ZD4054	1.78 ± 0.79‡	0/10	25 ± 2‡	22.4 ± 3.3‡
Paclitaxel	1.06 ± 0.82	0/10	31 ± 2‡	27.7 ± 2.2‡
ZD4054 + Paclitaxel	0.46 ± 0.1§	4/10	17 ± 2§	15.7 ± 3.3§

NOTE: Nude mice were given a s.c. injection of 1.5×10^6 viable HEY cells on day 0. Treatment was started on day 7 after tumor injection. Mice were treated for 21 d i.p. with ZD4054 (10 mg/kg/day) or with paclitaxel (20 mg/kg i.v. every 4 d for three doses) or with a combination of ZD4054 + paclitaxel. Mice were sacrificed on day 40 after tumor injection, and immunohistochemical analysis was performed. Each group consisted of 10 mice. No histological evidence of HEY tumor was detected in 4 of 10 mice treated with the combination of paclitaxel and ZD4054.

*Vessel counts were assessed by light microscopy after staining for CD31. Areas containing the highest numbers of capillaries and small venules were identified by scanning at low power, and individual vessel counts were performed at ×200.

†The relative number of proliferating cells was quantitatively assessed in 10 randomly selected fields (×200).

‡$P < 0.05$ compared with control.

§$P < 0.002$ compared with single treatments.

antagonist, ZD4054, to block ovarian cancer growth and progression. In ovarian carcinoma cells, pharmacological antagonism of ET_AR-driven autocrine pathways by ZD4054 resulted in a reduction of cell proliferation and angiogenic and invasive mediators, associated with elevated apoptotic signals. Furthermore, ZD4054 significantly antagonized ET_AR-associated proliferative and antiapoptotic signaling pathways, demonstrating the potential for inhibiting multiple tumor-promoting signals driven by ET_AR activation. Consistent with the *in vitro* results, ZD4054 affected the growth of HEY xenografts in nude mice leading to a significant reduction in tumor growth and neovascularization, with no associated toxicity. Current efforts to improve anticancer treatment are increasing, employing the concept of additive targets, such as the use of targeted agents in combination with cytotoxic drugs. This is critical in ovarian cancer, which, although highly responsive to platinum-based therapy after initial cytoreductive surgery, often recurs because of the emergence of drug resistance to conventional chemotherapy regimens (2). Novel therapeutic agents, in addition to combination regimens, may delay the emergence of resistance, thus prolonging remissions and improving long-term outcomes. In an attempt to understand the biological mechanisms underlying the drug response, we also evaluated the therapeutic efficacy of ZD4054 in combination with paclitaxel *in vitro* and *in vivo*. Consistent with previous results demonstrating the role of ET-1 as an antiapoptotic factor implicated in paclitaxel resistance (16), in the present study, we demonstrated that when the two agents were combined, a significant additive antitumor effect occurred compared to a single regimen, which was associated with a dramatic inhibition of the pleiotropic events triggered by ET_AR activation. The increased commitment toward apoptosis is dependent on the activation of caspase-3 and PARP and inactivation of the antiapoptotic bcl-2 protein, suggesting that ZD4054 may potentiate the antitumor activity of the cytotoxic agent paclitaxel by blocking survival pathways. The benefit of combining ZD4054 with paclitaxel becomes more pronounced following *in vivo* treatment, with complete regression of tumors in 40% of treated mice. The therapeutic efficacy of the combination of ZD4054 and paclitaxel is associated with a marked inhibition of tumor neovascularization and reduction in the proliferation index. In summary, our experiments demonstrated that ZD4054 enhances the antitumor effect of paclitaxel *in vivo*, highlighting the potential benefit of combining two therapeutic agents that have entirely different mechanisms of action. These results complement and extend previous studies published by our and other groups and support the concept that pharmacological blockade of the ET_AR using small molecule receptor antagonists in combination with cytotoxic drugs is therapeutically advantageous in different tumor types (21, 28–30, 40). Moreover, a recent gene expression profile analysis of intrinsic and/or acquired chemoresistance in ovarian cancers has identified the ET_AR as one of the genes highly expressed in postchemotherapy samples compared with untreated primary tumors, implicating this receptor as a target for prospective investigations of acquired chemoresistance in ovarian cancers (41). In conclusion, these findings have demonstrated the therapeutic efficacy of ZD4054, which has been shown to induce concomitant antitumor activity and inhibition of neovascularization, providing a rationale for the clinical evaluation of this molecule alone and in combination with cytotoxic drugs in patients with ovarian tumors.

Acknowledgments

We gratefully acknowledge Drs. Jim Growcott, Jon Curwen, and Nigel Brooks of AstraZeneca for kindly providing ZD4054; Stefano Masi, Valentina Caprara, Rocco Fraioli, and Aldo Lupo for help with the animal studies and excellent technical assistance; and Maria Vincenza Sarcone for secretarial assistance.

References

1. Jemal A, Siegel R, Ward E, et al. Cancer statistics 2006. CA Cancer J Clin 2006;56:106 – 30.

2. Agarwal R, Kaye SB. Ovarian cancer: strategies for overcoming resistance to chemotherapy. Nat Rev Cancer 2003;3:502 – 16.

3. Nelson J, Bagnato A, Battistini B, Nisen P. The endothelin axis: emerging role in cancer. Nat Rev Cancer 2003;3:110 – 6.

4. Bagnato A, Tecce R, Moretti C, Di Castro V, Spergel D, Catt KJ. Autocrine actions of endothelin-1 as a growth factor in human ovarian carcinoma cells. Clin Cancer Res 1995;1:1059 – 66.

5. Bagnato A, Salani D, Di Castro V, et al. Expression of endothelin-1 and endothelin A receptor in ovarian carcinoma: evidence for an autocrine role in tumor growth. Cancer Res 1999;59:720 – 7.

6. Bagnato A, Tecce R, Di Castro V, Catt KJ. Activation of mitogenic signaling by endothelin-1 in ovarian carcinoma cells. Cancer Res 1997;57:1306 – 11.

7. Rubanyi GM, Polokoff MA. Endothelins: molecular biology, biochemistry, pharmacology, physiology and pathophysiology. Pharmacol Rev 1994;4:325 – 415.

8. Donninger H, Bonome T, Radonovich M, et al. Whole genome expression profiling of advanced stage papillary serous ovarian cancer reveals activated pathways. Oncogene 2004;23:8065 – 77.

9. Bignotti E, Tassi RA, Calza S, et al. Gene expression profile of ovarian serous papillary carcinomas: identification of metastasis-associated genes. Am J Obstet Gynecol 2007;196:245.e1 – 11.

10. Salani D, Di Castro V, Nicotra MR, et al. Role of endothelin in neovascularization of ovarian carcinoma. Am J Pathol 2000;157:1537 – 47.

11. Bagnato A, Spinella F, Rosanò L. Emerging role of the endothelin axis in ovarian tumor progression. Endocr Relat Cancer 2005;12:761 – 72.

12. Rosanò L, Spinella F, Di Castro V, et al. Endothelin-1 promotes epithelial-to-mesenchymal transition in ovarian cancer cells. Cancer Res 2005;65:11649 – 57.

13. Spinella F, Rosanò L, Di Castro V, Nicotra MR, Natali PG, Bagnato A. Inhibition of cyclooxygenase-1 and -2 expression by targeting the endothelin A receptor in human ovarian carcinoma cells. Clin Cancer Res 2004;10:4670 – 9.

14. Vacca F, Bagnato A, Catt KJ, Tecce R. Transactivation of epidermal growth factor receptor in endothelin-1 – induced mitogenic signaling in human ovarian carcinoma cells. Cancer Res 2000;60:5310 – 7.

15. Rosanò L, Spinella F, Di Castro V, et al. Integrin-linked kinase functions as a downstream mediator of endothelin-1 to promote invasive behavior in ovarian carcinoma. Mol Cancer Ther 2006;5:833 – 42.

16. Del Bufalo D, Di Castro V, Biroccio A, et al. Endothelin-1 protects against paclitaxel-induced apoptosis: requirement for AKT activation. Mol Pharmacol 2002;61:524 – 32.

17. Spinella F, Rosanò L, Di Castro V, Natali PG, Bagnato A. Endothelin-1 induces vascular endothelial growth factor by increasing hypoxia inducible factor 1α in ovarian carcinoma cells. J Biol Chem 2002;277:27850 – 5.

18. Spinella F, Rosanò L, Di Castro V, Natali PG, Bagnato A. Endothelin-1 – induced prostaglandin E2 – 2, EP4 signaling regulates vascular endothelial growth factor production and ovarian carcinoma cell invasion. J Biol Chem 2004;279:46700 – 5.

19. Rosanò L, Varmi M, Salani D, et al. Endothelin-1 induces tumor proteinase activation and invasiveness of ovarian carcinoma cells. Cancer Res 2001;61:8340 – 6.

20. Spinella F, Rosanò L, Di Castro V, Nicotra MR, Natali PG, Bagnato A. Endothelin-1 decreases gap junctional intercellular communication by inducing phosphorylation of connexin 43 in human ovarian carcinoma cells. J Biol Chem 2003;278:41294 – 301.

21. Rosanò L, Spinella F, Salani D, et al. Therapeutic targeting of the endothelin a receptor in human ovarian carcinoma. Cancer Res 2003;63:2447 – 53.

22. Bagnato A, Cirilli A, Salani D, et al. Growth inhibition of cervix carcinoma cells in vivo by endothelin A receptor blockade. Cancer Res 2002;62:6381 – 4.

23. Kopetz ES, Nelson JB, Carducci MA. Endothelin-1 as a target for therapeutic intervention in prostate cancer. Invest New Drugs 2002;20: 173 – 82.

24. Bagnato A, Natali PG. Endothelin receptors as novel targets in tumor therapy. J Transl Med 2004;2:16.

25. Bradbury RH, Bath C, Butlin RJ, et al. New non-peptide endothelin-A receptor antagonists: synthesis, biological properties, and structure-activity relationships of 5-(dimethylamino)-*N*-pyridyl-,-*N*-pyrimidinyl-*N*-pyridazinyl-,and-*N*-pyrazinyl-1-naphthalenesulfonamides. J Med Chem 1997;40:996 – 1004.

26. Morris CD, Rose A, Curwen J, Hughes AM, Wilson DJ, Webb DJ. Specific inhibition of the endothelin A receptor with ZD4054: clinical and pre-clinical evidence. Br J Cancer 2005;92:2148 – 52.

27. Rosanò L, Di Castro V, Spinella F, Decandia S, Natali PG, Bagnato A. ZD4054, a potent endothelin receptor A antagonist, inhibits ovarian carcinoma cell proliferation. Exp Biol Med (Maywood) 2006;231:1132 – 5.

28. Rosanò L, Spinella F, Di Castro V, Natali PG, Bagnato A. Therapeutic targeting of the endothelin-A receptor in human ovarian carcinoma: efficacy of cytotoxic agents is markedly enhanced by co-administration with atrasentan. J Cardiovasc Pharmacol 2004;44:S132 – 5.

29. Akhavan A, McHugh KH, Guruli G, et al. Endothelin receptor A blockade enhances taxane effects in prostate cancer. Neoplasia 2006;8: 725 – 32.

30. Banerjee S, Hussain M, Wang Z, et al. In vitro and in vivo molecular evidence for better therapeutic efficacy of ABT-627 and taxotere combination in prostate cancer. Cancer Res 2007;67:3818 – 26.

31. Weidner N, Semple JP, Welch WR, Folkman J. Tumor angiogenesis and metastasis-correlation in invasive breast carcinoma. N Engl J Med 1991;324:1 – 8.

32. Venuti A, Salani D, Manni V, Poggiali F, Bagnato A. Expression of endothelin-1 and endothelin A receptor in HPV-associated cervical carcinoma: new potential targets for anticancer therapy. FASEB J 2000; 14:2277 – 83.

33. Gohji K, Kitazawa S, Tamada H, Katsuoka Y, Nakajima M. Expression of endothelin receptor a associated with prostate cancer progression. J Urol 2001;165:1033 – 6.

34. Wulfing P, Diallo R, Kersting C et al. Expression of endothelin-1, endothelin-A, endothelin-B receptor in human breast cancer and correlation with long-term follow-up. Clin Cancer Res 2003;9:4125 – 31.

35. Egidy G, Juillerat-Jeanneret L, Jeannin JF, et al. Modulation of human colon tumor-stromal interactions by the endothelin system. Am J Pathol 2000;157:1863 – 74.

36. Ahmed SI, Thompson J, Coulson JM, Woll PJ. Studies on the expression of endothelin, its receptor subtypes, and converting enzymes in lung cancer and in human bronchial epithelium. Am J Respir Cell Mol Biol 2000;22:422 – 31.

37. Douglas ML, Richardson MM, Nicol DL. Endothelin axis expression is markedly different in the two main subtypes of renal cell carcinoma. Cancer 2004;100:2118 – 24.

38. Donckier JE, Michel L, Van Beneden R, Delos M, Havaus X. Increased expression of endothelin-1 and its mitogenic receptor ETA in human papillary thyroid carcinoma. Clin Endocrinol (Oxf) 2003;59:354 – 60.

39. Guise TA. Molecular mechanisms of osteolytic bone metastases. Cancer 2000;88:2892 – 8.

40. Hai-Qiang Mai, Zong-Yuan Zeng, Kai-Tao Feng, et al. Therapeutic targeting of the endothelin a receptor in human nasopharyngeal carcinoma. Cancer Sci 2006;97:1388 – 95.

41. Jazaeri AA, Awtrey CS, Chandramouli GV, et al. Gene expression profiles associated with response to chemotherapy in epithelial ovarian cancers. Clin Cancer Res 2005;11:6300 – 10.